

## Assessment of predictive capabilities of SST-based Detached Eddy Simulation for incompressible flow over an open cavity

*Kyongsik Chang*<sup>1</sup>, *George Constantinescu*<sup>2</sup> and *Seung-O Park*<sup>3</sup>

1. KAIST, Daejeon 305-701, South Korea, [kschang76@kaist.ac.kr](mailto:kschang76@kaist.ac.kr)

2. Civil and Environmental Engineering Department and IIHR Hydrosience and Engineering, The University of Iowa, Iowa city, IA 52242, USA, [sconstan@engineering.uiowa.edu](mailto:sconstan@engineering.uiowa.edu)

3. KAIST, Daejeon 305-701, South Korea, [sopark@kaist.ac.kr](mailto:sopark@kaist.ac.kr)

*Corresponding author Kyongsik Chang*

### Abstract

The three-dimensional (3D) incompressible flow past an open cavity in a channel is investigated using an SST based version of Detached Eddy Simulation (DES) and with an SST Unsteady RANS (URANS) model. The length to depth ratio of the cavity is two, and the flow upstream the cavity is fully turbulent. Sensitivity of DES predictions to the presence of fluctuations in the inflow section is also investigated. The predictive abilities of DES and URANS are assessed based on comparison with results from a well resolved LES simulation conducted on a very fine mesh. Particular attention is given to assessing the performance of these less expensive methods in correctly predicting the mass exchange between the passive scalar initially situated inside the cavity and the surrounding flow.

**Keywords:** *Open cavity, Detached Eddy Simulation, Large Eddy Simulation*

### 1. Introduction

Cavity flows are relevant for many engineering applications, for example in the bomb bay and landing systems of aircrafts. In these flows the effect of pressure and velocity oscillations is to generate aero-acoustic noise and vibrations that can eventually increase the fatigue of the structures. For environmental applications, which are the focus of the present study, the presence of cavity-like geometries in rivers, lakes or urban canyons especially under stratified conditions, may adversely affect the water / air quality when pollutants can accumulate in these cavities. The main difference with the cavity flows typically encountered in aerodynamics flows is that the flow is incompressible and fully turbulent upstream the cavity. Also, the quantitative characterization of the mass exchange between the cavity and the surrounding is highly important. Though many experimental and numerical investigations of cavity flows are available, most of them focused on the compressible case with a developing laminar or turbulent incoming boundary layer. For quasi incompressible flows, Sarohia [1] studied experimentally the flow around an axisymmetric cavity and measured the minimum cavity length for oscillations to occur over the cavity. He observed that the frequency of the main oscillations switched to a higher mode as the length was increased. Rockwell and Naudasher [2] predicted the main oscillatory frequency for incompressible flow over 2D cavities based on linear stability theory. As far as eddy resolving simulations of incompressible cavity flows, one should mention the study of Yao *et al.* [3] who used LES to calculate the flow past a three dimensional cavity at cavity Reynolds number between 5,000 and 50,000 with laminar inflow conditions.

### 2. Numerical method, computational domain, grid generation and flow conditions

The 3D incompressible Navier-Stokes equations are integrated using a fully implicit fractional step method [4]. The governing equations are transformed to generalized curvilinear coordinates on a non-staggered grid. Convective terms in DES are discretized using a blend of fifth-order accurate upwind biased scheme and second-order central scheme following Travin *et al.* [5] to minimize the level of numerical dissipation away from solid boundaries. The blending function  $\sigma$  proposed in [5] is

used. For URANS, the second order upwind scheme is used. All other terms in momentum and pressure-Poisson equations are approximated using second-order central differences. Time integration is done using a double time stepping algorithm and local time stepping is used to accelerate the convergence. The SST model is used in URANS to allow a direct comparison with DES for which the SST version [6] is used. The DES formulation of SST is obtained by redefining the length scale ( $l_{SST}$ ) in dissipation term of the transport equation for the modeled t.k.e. by  $l_{DES} = \min(l_{SST}, C_{DES}\Delta)$  such that away from solid boundaries the turbulence length scale is proportional to the local grid size  $\Delta$  as in LES. The model parameter  $C_{DES}$  is obtained from  $C_{DES} = (1-F_1)C_{DES}^{k-\epsilon} + F_1C_{DES}^{k-\omega}$  using the blending function  $F_1$  proposed by Menter [6], the values of  $C_{DES}^{k-\epsilon}$  and  $C_{DES}^{k-\omega}$  are 0.61 and 0.78 respectively.

The length to depth ratio ( $L/D$ ) of the cavity is 2 and the Reynolds number defined with the cavity depth and the mean velocity in the upstream channel is 3,360, corresponding to the experiments in [7]. A sketch of the computational domain is provided in Fig. 1. The length of the domain in the spanwise direction is equal to  $2D$  and periodic conditions are employed in this direction. The computational domain in DES and URANS consists of close to 500,000 mesh points which is sensible less than the mesh used in the previous well resolved LES simulation (14 million mesh points) at same Reynolds number. The first point off wall is located everywhere at about one wall unit away from the walls and no wall functions are used. The nondimensional time step is  $0.02D/U$  which corresponds to about 125 time steps for one shedding period of the large spanwise vortices over the cavity.

Special attention was given to the study of the sensitivity of the solution to the upstream boundary conditions. Though in many applications in which DES is used it is not necessary to superimpose fluctuations at the inflow, the effect of the presence of these fluctuations on the momentum and mass exchange over the top of the cavity is not well understood. To investigate these effects, two DES simulations were run. In the first one a precalculated fully developed SST steady RANS solution was specified at the channel inflow, while in the second one the instantaneous velocity components were fed in a time accurate way through the inflow sections. The instantaneous velocities containing real turbulence fluctuations were obtained from a precalculated LES solution in a channel of identical section at same Reynolds number (same data fields used to specify the inflow conditions in the well resolved LES solution in [8] used for validation). This LES data was interpolated in both space and time corresponding to the grid and time step used in DES. In URANS, same profiles corresponding to the fully developed SST channel solution were used to specify inflow conditions.

### 3. Results and discussion

Comparison of URANS and DES solution with no fluctuations at the inlet (DES-R) allow us to assess whether a hybrid RANS/LES approach like DES can predict the mean quantities, turbulence statistics and mass exchange processes more accurately than URANS for flows over cavities. Comparison of the DES solution without (DES-R) and with (DES-L) realistic turbulence fluctuations at the inflow allow us to understand what is the added benefit of having the solution jittered at the inflow in terms of improving the overall flow, turbulence statistics and global mass exchange coefficient predictions. The particular kind of jittering applied here (from a well resolved LES solution) is an extreme case as it is closest to what we can call realistic turbulence. In many cases it is too expensive to calculate such a solution and simpler methods that include generation of synthetic turbulence or just adding random fluctuations can be used. However, the benefit of using these methods is expected to be lower than using the jittering employed in DES-L. The predictive capabilities of all these three approaches are quantitatively assessed by comparison with the results of the well resolved LES simulation of the same flow where the resolution was close to DNS requirements, and thus most of the energy was resolved. The URANS and DES-R solutions were started using one of the instantaneous DES-L flow fields in which the unsteady flow over the cavity was well established. The first observation is the fact that while as expected both DES solutions predicted an unsteady flow over the cavity characterized by the shedding of fairly large spanwise vortices from the leading edge of the cavity, the URANS solution predicted a steady solution. It is expected that adding velocity fluctuations in the inflow section [7] may force the shear layer on top of the cavity to start shedding vortices and thus to obtain an unsteady solution however, as the focus of the present paper is DES, this approach was not pursued.

## Assessment of predictive capabilities of SST-based Detached Eddy Simulation for incompressible flow over an open cavity

All four simulations show that the mean flow inside the cavity is characterized by the presence of two main recirculation eddies (see Fig. 2), with the larger one occupying the whole downstream half of the cavity and part of the top upstream half. However, the relative size and shape of these main eddies are not exactly the same, with URANS predicting a shallower upstream eddy compared to LES and the two DES simulations. Figure 3 shows the evolution of the mean shear layer thickness defined with the vorticity thickness ( $\delta_w = U / (dU/dy)_{\max}$ ). This quantity allows comparison of the mean shear layer characteristics on top of the cavity among the models. The vorticity thickness increases starting at the leading edge over most of the cavity and then decreases rapidly as the trailing edge is approached. The vorticity thickness in LES varies linearly between  $6\delta_{w0}$  and  $13\delta_{w0}$ , where  $\delta_{w0}$  is the vorticity thickness at the leading edge. The growth rate is close to 0.27 in the linear growth region. In the linear growth region, the growth rates predicted by DES-L and DES-R are 0.26, very close to LES, whereas URANS overpredicts the growth rate at 0.31. Moreover, near the trailing edge URANS significantly overpredicts the thickness of the shear layer. As expected, DES-L appears to give the closest variation of this quantity over the cavity when compared to LES. The total (resolved plus modeled) t.k.e. contours are compared in Fig. 4. In LES, t.k.e. increases significantly inside the shear layer and over the top part of the downstream cavity wall due to the presence of highly energetic vortical structures in the detached shear layers and their subsequent interaction with the trailing edge, where part of them are convected inside the cavity. URANS underpredicts the t.k.e. levels especially in the upstream part of the detached shear layer (remember URANS solution is steady thus no vortices are shed) and inside the cavity. Unexpectedly, DES-R underpredicts the t.k.e. inside these regions even more than URANS. DES-L predictions are remarkably close to LES over the whole domain surrounding the cavity which shows that, with the right level of upstream fluctuations, DES can predict t.k.e. as well as LES but at a fraction of the cost associated with well resolved LES.

Power spectra of vertical velocity at a point situated on top of the cavity close to the trailing edge are shown in Fig. 5 for DES and LES (recall URANS predicted a steady solution). As expected, LES predicts the presence of a broad spectrum inside the shear layer where the turbulence intensity is substantially increased relative to the surrounding flow. The range of energetic frequencies corresponds to Strouhal numbers  $St = fU/D$  between 0.05 and 1 with the most energetic frequency at  $St = 0.38$  corresponding to the first mode predicted in [2] for cavities with  $L/D = 0.2$ . A secondary peak is observed in the spectrum at  $St = 0.51$  which corresponds to the second mode predicted in [2]. This is the dominant mode in the case in which the incoming boundary layer is laminar and is associated with the shedding of the vortex tubes in the detached shear layers. However, in the turbulent case, these spanwise structures are not so dominant and most of their coherence is destroyed due to the interaction of the vorticity in the detached shear layer with the eddies convected in the channel from upstream. In the case of DES-R though the mean profile in the channel corresponds to fully turbulent flow, the absence of upstream fluctuations makes the flow over the cavity to resemble more to the one observed past a cavity with an incoming steady (laminar) boundary layer where the unsteadiness is due to the quasi-periodic shedding of spanwise vortices. These vortices eventually get disturbed as they approach the trailing edge where secondary instabilities force transition to 3D. This is clearly observed in the visualization of the instantaneous vortical structures deduced using the Q criterion in Fig. 7a. The transition from 2D to 3D in the downstream half of the cavity is also inferred from the out of plane instantaneous vorticity contours. In the spanwise  $y-z$  plane at  $x/D = 1$  (Fig. 6a) three recirculation cells and the associated spanwise disturbances of the top shear layer are observed. In the vorticity contours in the  $x-z$  plane in the same figure, two distinct spanwise vortices are observed. They are shed quasi regularly with a frequency of  $St = 0.31$  as observed in Fig. 5b. On the same plot a secondary peak at  $St = 0.62$  corresponding to the first harmonic of the fundamental shedding frequency indicates the presence of strong non-linear interactions among the eddies in the detached layer. In the case when upstream fluctuations are present in the incoming flow, the flow structure changes significantly in the sense that the intensity of the resolved 3D eddies in the detached layer and especially inside the cavity is larger compared to DES-R. In DES-L case the vorticity plots at  $x/D = 1$  indicate the presence of a 3D flow dominated by random eddies instead of the rather organized motions present in DES-R. Even though the shedding frequency  $St = 0.31$  is the same and the coherence of the spanwise vortices (Fig. 5c) remains fairly strong (these vortices are easily observable in  $xz$  plane in Fig. 6b) the intensity of the disturbances that deform these structures is clearly larger compared to DES-R (Fig 7b). The jittering of the spanwise vortices introduces very irregular

interactions between these vortices and the trailing edge over the span, which produces pressure disturbances that propagate upstream and further jitter the vortex tubes near the leading edge. Consistent with the broader range of scales observed in Figs. 6b and 7b, the spectra at the same point show the presence of a continuous band of energetic frequencies between  $St=0.1$  and  $0.55$ . Though the shedding frequency at  $St=0.31$  is still the most energetic, a secondary energetic frequency associated with the second mode predicted in [2] is present consistent with the spectrum measured in the well resolved LES. This clearly shows that if the spectral content of the flow is relevant for the investigation, adding turbulent fluctuations that mimic as close as possible the real turbulence can help in improving the DES predictions. Still, even without any upstream fluctuations, DES produces an unsteady solution with resolved eddies that are clearly turbulent over the downstream cavity half.

Fig. 8 shows the decay of the scalar mass inside the cavity. The scalar was introduced instantaneously over the whole cavity once the flow was statistically steady. The simulation was then continued until the scalar was purged from the cavity. The Schmidt number was equal to 1. In environmental engineering, global 1D models [9] relying on empirical dispersion coefficients are used to describe the mass exchange between the cavity and the main channel. These models simply assume that the local rate of decay of pollutant mass inside the cavity is proportional to the mean concentration difference between the channel and cavity. If this law is assumed, then the decay of scalar mass inside cavity is exponential  $M/M_0=\exp(-t/T)$  where  $T$  is the characteristics time scale,  $M_0$  is the initial mass of scalar. If one nondimensionalizes  $T$  using  $D$  and  $U$ , one gets the so-called nondimensional exchange coefficient  $k$ . A constant value of  $k$  corresponds to a linear variation of the total mass in time in log-log scale. As observed in Fig. 8 the decay in all the four simulations can be considered as linear in a good approximation. However, if the corresponding value of  $k$  is  $0.015$  in LES, both DES simulations predict  $k$  close to  $0.013$  which suggest that the added fluctuations did not affect substantially the exchange process. On the other hand, the steady URANS solution severely underpredicts the mass exchange coefficient, the inferred value of  $k$  being close to  $0.009$ . This translates into a time of  $260D/U$  for 90% of the scalar to leave the cavity in URANS compared to only  $170D/U$  in LES. The reasons for that are evident by comparing the instantaneous scalar distribution over the duration of the purging process in Fig. 9. In DES-L the resolved eddies in the detached shear layer are regularly engulfing fluid from the downstream recirculation eddy containing a high scalar concentration. This process speeds up the overall mixing and is absent from the steady URANS solution where the scalar is first ejected (frames a to d in Fig. 9a) from the downstream part of the cavity (downstream recirculation eddy) after which, very slowly, scalar from the upstream recirculation eddy is entrained out of the cavity. In DES-L due to the spanwise instabilities and 3D eddies present in the cavity, the scalar mass exchange is much more irregular (Fig. 9b) and the scalar concentration decays over the whole cavity even in the initial phase of the purging process.

#### 4. Conclusions

The 3D flow past a rectangular 2D cavity in a channel was investigated using an SST-based version of DES and URANS. Two DES simulations one without fluctuations and one with realistic turbulence fluctuations were performed to investigate to what degree the presence of these fluctuations can improve the predictions compared to those of a well resolved LES simulation. While URANS predicted a steady solution, DES with same steady inflow conditions predicted an unsteady solution dominated by the shedding of quasi 2D spanwise vortices in the detached shear layer followed by transition to 3D. The resolved flow remained practically laminar. Adding turbulence fluctuations at the inlet induced large 3D disturbances inside the detached shear layer and in the downstream part of the cavity. The intensity of these motions was, as expected, lower than in LES. However, the difference between the flow fields in the two DES simulations appeared to have a very small effect on the overall mass exchange process between the cavity and the surroundings. In contrast, URANS was found to significantly underestimate the global mass exchange coefficient relative to LES.

#### References

- [1] Sorojia, V., "Experimental investigation of oscillation in flows over shallow cavities", *AIAA J.*, Vol. 15, (1977), pp 984-991.

**Assessment of predictive capabilities of SST-based Detached Eddy Simulation for incompressible flow over an open cavity**

- [2] Rockwell, D. and Naudascher, E., "Review - self-sustaining oscillations of flow past cavities", *J. Fluids Engrg.*, Vol. 100, (1978), pp 152-165.
- [3] Yao H., Copper R.K. and Raghunthan S.R., "Large-eddy simulation of laminar-to-turbulent transition in incompressible flow past 3-D rectangular cavity," *AIAA paper*, 2001-31318. (2001).
- [4] Constantinescu G. and Squires K., "Numerical investigations of flow over a sphere in the subcritical and supercritical regimes", *Physics of Fluids*, Vol. 16, No. 5, (2004), pp 1449-1466.
- [5] Travin A., Shur M., Strelets M., and Spalart P.R., "Physical and numerical upgrades in the detached-eddy simulation of complex turbulent flows", *In: 412 EUROMECH Colloquium on LES of Complex transitional and turbulent flows*, Munich, Oct. (2000).
- [6] Menter P.R., "Zonal two-equation  $k-\omega$  turbulence models for aerodynamic flows," *AIAA paper*, 1993-2906. (1993).
- [7] Pereira, J. C. F., and Sousa, J. M. M., "Experimental and numerical investigation of flow oscillations in a rectangular cavity", *J. Fluids Engrg.*, Vol. 117, (1995), pp 68-73.
- [8] Chang K., Constantinescu S. G. and Park S., "Influence of inflow conditions on the development of the flow and pollutant transport for the flow past an open cavity", *4<sup>th</sup> ICCHMT*, Cachan, France, No. 128, (2005).
- [9] Uijtewaal, W. S. J, Lehmann, D., and van Mazijk, "Exchange processes between a river and its groyne fields: Model experiments", *J. Hydraulic Engrg.*, Vol. 127, (2001), pp 928-936.

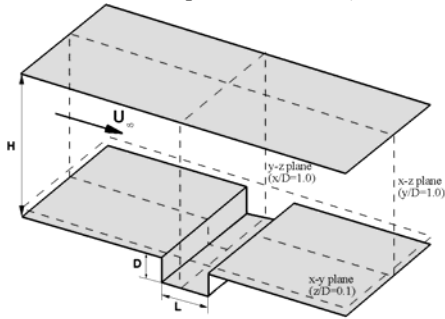


Fig. 1. Computational domain

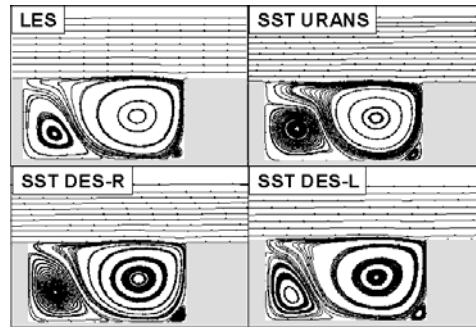


Fig. 2. Mean 2D streamlines.

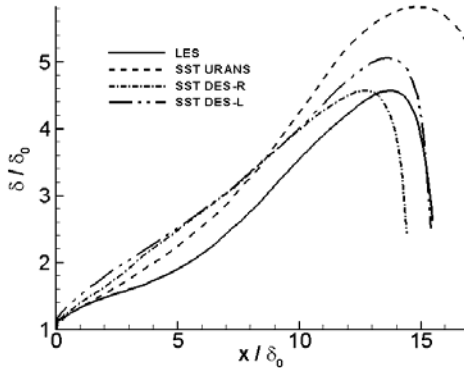


Fig. 3. Shear-layer vorticity thickness( $\delta_{\omega}$ ) variation with distance from leading edge.

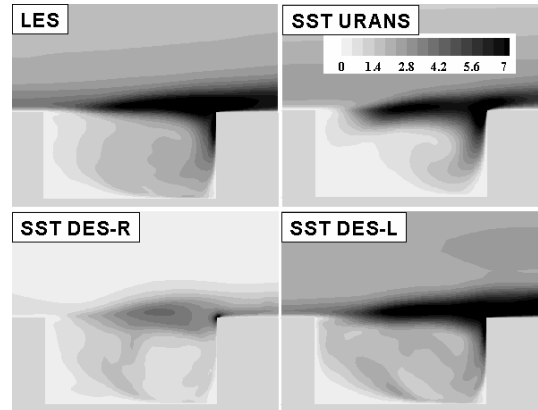


Fig. 4. Total (resolved plus modeled) t.k.e. contours.

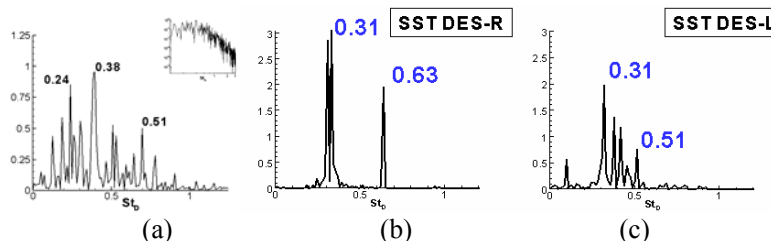


Fig. 5. Power spectra of the vertical velocity at  $(x/D, y/D)=(1.8, 0.0)$ . (a)LES; (b)DES-R; (c)DES-L.

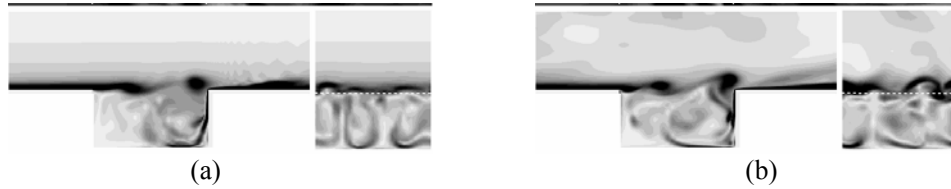


Fig. 6. Out-of-plane instantaneous vorticity magnitude in representative planes (see Fig. 1 for relative position of planes). (a) DES-R; (b) DES-L.

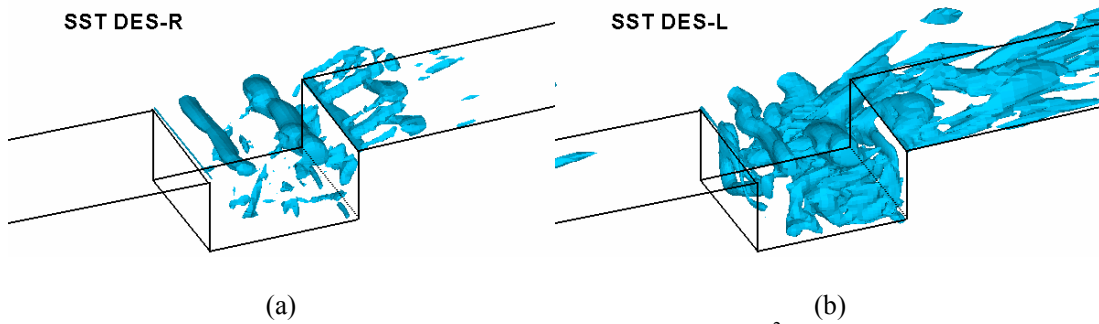


Fig. 7. Instantaneous vortical structures using Q-criterion,  $Q/(U_\infty/L)^2=0.5$ . (a)DES-R; (b)DES-L.

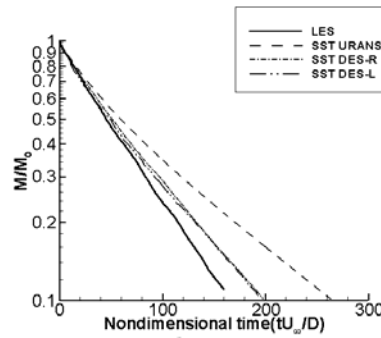


Fig. 8. Decay of scalar mass inside the cavity (log-log scale).

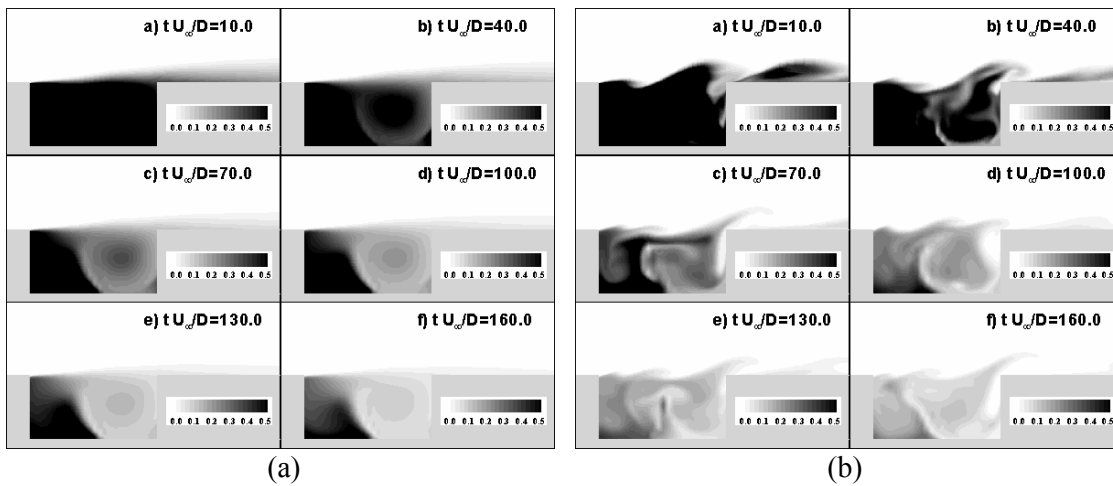


Fig. 9. Instantaneous contours of passive scalar concentration. (a) URANS; (b)DES-L.